Nanoscale

PAPER

View Article Online
View Journal | View Issue

Cite this: *Nanoscale*, 2016, **8**, 10096

Three-dimensional quick response code based on inkjet printing of upconversion fluorescent nanoparticles for drug anti-counterfeiting†

Minli You,[a,b] Min Lin,*[a,b] Shurui Wang,[a,b] Xuemin Wang,[a,b] Ge Zhang,[b] Yuan Hong,[b] Yuqing Dong,[a,b] Guorui Jin[a,b] and Feng Xu*[a,b]

Received 17th February 2016,
Accepted 14th April 2016

DOI: 10.1039/c6nr01353h

www.rsc.org/nanoscale

Medicine counterfeiting is a serious issue worldwide, involving potentially devastating health repercussions. Advanced anti-counterfeit technology for drugs has therefore aroused intensive interest. However, existing anti-counterfeit technologies are associated with drawbacks such as the high cost, complex fabrication process, sophisticated operation and incapability in authenticating drug ingredients. In this contribution, we developed a smart phone recognition based upconversion fluorescent three-dimensional (3D) quick response (QR) code for tracking and anti-counterfeiting of drugs. We firstly formulated three colored inks incorporating upconversion nanoparticles with RGB (*i.e.*, red, green and blue) emission colors. Using a modified inkjet printer, we printed a series of colors by precisely regulating the overlap of these three inks. Meanwhile, we developed a multilayer printing and splitting technology, which significantly increases the information storage capacity per unit area. As an example, we directly printed the upconversion fluorescent 3D QR code on the surface of drug capsules. The 3D QR code consisted of three different color layers with each layer encoded by information of different aspects of the drug. A smart phone APP was designed to decode the multicolor 3D QR code, providing the authenticity and related information of drugs. The developed technology possesses merits in terms of low cost, ease of operation, high throughput and high information capacity, thus holds great potential for drug anti-counterfeiting.

Introduction

Anti-counterfeit technologies for products have been widely used in the market, while traditional anti-counterfeit technologies are easily infringed. An advanced anti-counterfeit technology is therefore urgently needed in many important fields, especially for anti-counterfeit of drugs.[1] The World Health Organization (WHO) reports 10% of the global pharmaceutical trade (as high as 25% in developing countries) is counterfeit,[2] which causes the total loss of life between 500 000 and 1 000 000 people per year.[3] To address this issue, significant efforts have been devoted to the development of advanced technologies for anti-counterfeiting of drugs, which should be hard to duplicate, easy to prepare, high throughput, convenient to recognize and inexpensive. For instance, radio frequency identification (RFID) based on electromagnetic fields to transfer drug authentication data is one of the emerging technologies for drug anti-counterfeiting. It features the advantages of its trackability, high information capacity and contactless recognition.[4] However, its high cost (>$25 for active tags, 7–15 cents for passive tags)[5] limits its practical usage and its rewritability threatens the safety of the stored information. Holography that can display a fully 3D image of a holographed subject is commonly used as a security feature on products including drugs.[6] However, holographic technology is complex and depends on expensive manufacturing equipment. In addition, most existing anti-counterfeit technologies perform their functions by tagging on the drug packaging, which is easy to exchange shoddy drugs for quality drugs by unscrupulous traders. Therefore, it remains a challenge to develop a low cost, highly safe and convenient technology for tracking and anti-counterfeiting of drugs.

To this end, the QR code has been used for anti-counterfeit technology[7,8] and the lithography based QR code has been recently developed for the tracking and anti-counterfeiting of

[a]*The Key Laboratory of Biomedical Information Engineering of Ministry of Education, School of Life Science and Technology, Xi'an Jiaotong University, Xi'an 710049, P.R. China. E-mail: minlin@mail.xjtu.edu.cn, fengxu@mail.xjtu.edu.cn*
[b]*Bioinspired Engineering and Biomechanics Center (BEBC), Xi'an Jiaotong University, Xi'an 710049, P.R. China*

†Electronic supplementary information (ESI) available: Calculating details of UCNP content per 3D QR code and decoding process of the 3D QR code. See DOI: 10.1039/c6nr01353h

drugs by smartly incorporating an encoded polymer microtaggant into a single capsule.[9] Nevertheless, the lithography based QR code requires a complicated fabrication process and a microscope is needed to manually recognize the micro-sized tag. Besides lithography, many other technologies have also been developed to fabricate QR codes, such as laser engraving,[10,11] screen-printing[12] and inkjet printing.[13] Among these, inkjet printing offers several advantages, such as high throughput, designability, low cost and ease of fabrication.[13–17] However, the ease in duplication of current visible QR codes hinders their widespread applications in drug anti-counterfeiting.[18,19]

To address this issue, a fluorescent QR code has been developed using various fluorescent materials (*e.g.*, quantum dots, carbon dots and organic dyes).[20,21] Although these materials offer high fluorescence emission intensity and precisely tunable excitation/emission wavelengths, they are partly limited by photobleaching, poor photostability, high background noise and easy duplication.[22] Upconversion nanoparticles (UCNPs) that are capable of converting multiple low energy photons to one higher energy photon can be an excellent candidate for the fabrication of fluorescent QR codes.[23] In addition, UCNPs and near infrared (NIR) excitation sources are difficult to access, making the upconversion fluorescent QR code harder to duplicate.[7] Moreover, UCNPs are associated with unique optical features including robust photostability, long fluorescence life, low background noise and multicolors.[24] In addition, the design of a multilayer QR code with better security and accompanying higher capacity potentiates excellent anti-counterfeiting merits.[25]

In this study, we reported an upconversion fluorescent based 3D QR code fabricated by inkjet printing technology for drug anti-counterfeiting. Firstly, RGB colored printing inks of UCNPs were synthesized and the printed color was precisely tuned by controlling the ratio overlapped with RGB upconversion inks. Then, we printed the 3D QR code composed of RGB color upconversion inks on the surface of drug capsules. A specialized smart phone application (APP) was developed to decode the complicated 3D QR code, providing a basic description of the drug, picture of drug packaging and website of the drug manufacturer. Subsequently, authenticity and related information of the drugs were verified by the obtained information from the 3D QR code. The developed user-friendly technology possesses merits in terms of high throughput, high information capacity, low cost, and could be widely used as a powerful and convenient method for various anti-counterfeiting applications.

Materials and methods

Materials

$YCl_3{\cdot}6H_2O$, $YbCl_3{\cdot}6H_2O$, $ErCl_3{\cdot}6H_2O$, $TmCl_3{\cdot}6H_2O$, and ammonium fluoride (NH_4F) were purchased from Sigma Aldrich and used as received. 1-Octadecene (90%) and oleic acid (90%) were purchased from Alfa Aesar. Methanol, cyclohexane, ethanol, glycerol (99.0%) and sodium hydroxide (NaOH) were purchased from Tianjinzhiyuan Chemical Reagent Co., Ltd. Poly(acrylic acid) (PAA, M_w = 1800) was purchased from Tianjinyongsheng Chemical Reagent Co., Ltd. Sodium dodecyl sulfate (SDS) was bought from ChengDu Kelong Chemical Co., Ltd. Ultrapure water was prepared from a Milli-Q Integral Water Purification System (resistance >18 MΩ cm^{-1}). All reagents were of analytical grade and used without any purification.

Synthesis of RGB UCNPs

The synthesis of UCNPs was carried out following literature procedures.[26,27] In a typical synthesis process of β-$NaYF_4$:2% Er,18% Yb, a mixture of 7.5 mL oleic acid and 15 mL 1-octadecene was firstly added into a 100 mL flask and stirred. Subsequently, a 2 mL precursor solution composed of 0.8 mmol $YCl_3{\cdot}6H_2O$, 0.18 mmol $YbCl_3{\cdot}6H_2O$, and 0.02 mmol $ErCl_3{\cdot}6H_2O$ was added dropwise. After 30 minutes of stirring, the mixture was heated to 120 °C for 1 hour and 156 °C for another 1 hour to get rid of water with protection of an argon atmosphere. Then 4 mmol NH_4F and 2.5 mmol NaOH were dissolved in 10 mL methanol and the resulting solution was added to the mixture that had been cooled down to room temperature. The mixture was heated to 110 °C for 1 hour to get rid of methanol. Then, the mixture was directly heated to 280 °C and kept for 1.5 hours. The resulting product was obtained after centrifugation at 10 000 revolutions per minute (rpm) for 10 minutes and washed with ethanol several times. To synthesize red and blue UCNPs, only the amounts of precursors were changed as follows: 1.76 mmol $YCl_3{\cdot}6H_2O$, 0.36 mmol $YbCl_3{\cdot}6H_2O$, 0.2 mmol $ErCl_3{\cdot}6H_2O$, 0.04 mmol $TmCl_3{\cdot}6H_2O$ for $NaYF_4$:10% Er,2% Tm and 1.494 mmol $YCl_3{\cdot}6H_2O$, 0.5 mmol $YbCl_3{\cdot}6H_2O$, 0.006 mmol $TmCl_3{\cdot}6H_2O$ for $NaYF_4$:25% Yb,0.3% Tm.

Surface modification of UCNPs

To make UCNPs water-soluble, a hydrophilic ligand, poly (acrylic acid), was used for modification of the UCNP surface. 158 mg PAA dissolved in 1 mL ethanol was mixed with 1 mL chloroform solution containing 15 mg UCNPs. The mixture was kept under stirring for 24 hours. Then, the obtained solution was washed several times using ultrapure water and finally dispersed in water.

Formulation of RGB inks and printing on the surface of drug capsules

The hydrophilic RGB inks were produced according to our previous reported method.[13] 15 mg PAA coated UCNPs were added to a 3 mL solution mixed with 70% ethanol (10%) and 30% glycerol solution. Then, 3 mg L^{-1} SDS was added to the mixture to obtain an appropriate surface tension and dynamic viscosity for an inkjet printer. Finally, the obtained mixture was in alternation with sonication and vortex for 10 minutes and stored in 4 °C for use. For printing of the 3D QR code on the drug capsule surface, capsule shells were first flattened after removing the inner drug powder. Then, the flattened

capsule shells were pasted on A4 paper and printed with pre-designed 3D QR code patterns. The obtained capsule shells recovered their shape with the assistance of a cotton swab. After reloading the drug powder, a drug capsule with the 3D QR code was finally obtained.

Characterization

A modified Canon iX6580 inkjet printer was used for inkjet printing. HT7700 transmission electron microscopy was used for the morphology characterization of samples under an accelerating voltage of 100 kV. The fluorescence spectra were recorded with a QuantaMasterTM40 spectrophotometer equipped with a 250 mW 980 nm laser diode (RGB Laser Systems). Images of printed patterns were firstly taken by using a Nikon D90 camera with an IR filter under excitation of a 980 nm CW laser (Changchun Liangli Photoelectric Co., Ltd). The images from the camera were then transferred to an android phone and followed by the decoding processes with a self-developed APP in the android phone. All the measurements were performed at room temperature.

Results and discussion

Drug counterfeiting is a serious issue worldwide, involving potentially devastating health repercussions, which calls for an advanced anti-counterfeit technology. However, the existing anti-counterfeit technologies are lacking authentication for the drug ingredients, and are not user-friendly making them hard for consumers to access. Herein, we developed a smart phone recognizable upconversion fluorescent 3D QR code as an advanced anti-counterfeit technology, which features high security, tracking and anti-counterfeiting of drugs, convenience and ease of use. Using a modified inkjet printer, we printed three multicolor layers encoded with different drug information on the surface of drug capsules (or tablets) (Fig. 1a). Inkjet printing technology makes the upconversion fluorescent 3D QR code easy for massive production and high throughput. No visible patterns can be observed after the 3D QR code was printed on the surface of capsules, resulting in an improved anti-counterfeiting effect. The multilayered QR code with different colors on the drug surface can be recognized by using a smart phone only under excitation of a 980 nm laser (Fig. 1b). To decode the complicated 3D QR code, we designed a specific APP, which can directly convert the 3D code to 3 recognizable black/white 2D QR codes and further verify the information of drugs such as the authenticity and validity period (Fig. 1c).

Upconversion nanoparticles excited by 980 nm wavelength possess unique properties of robust photostability, scale up capability, long fluorescence life and low background noise, which are suitable for anti-counterfeiting.

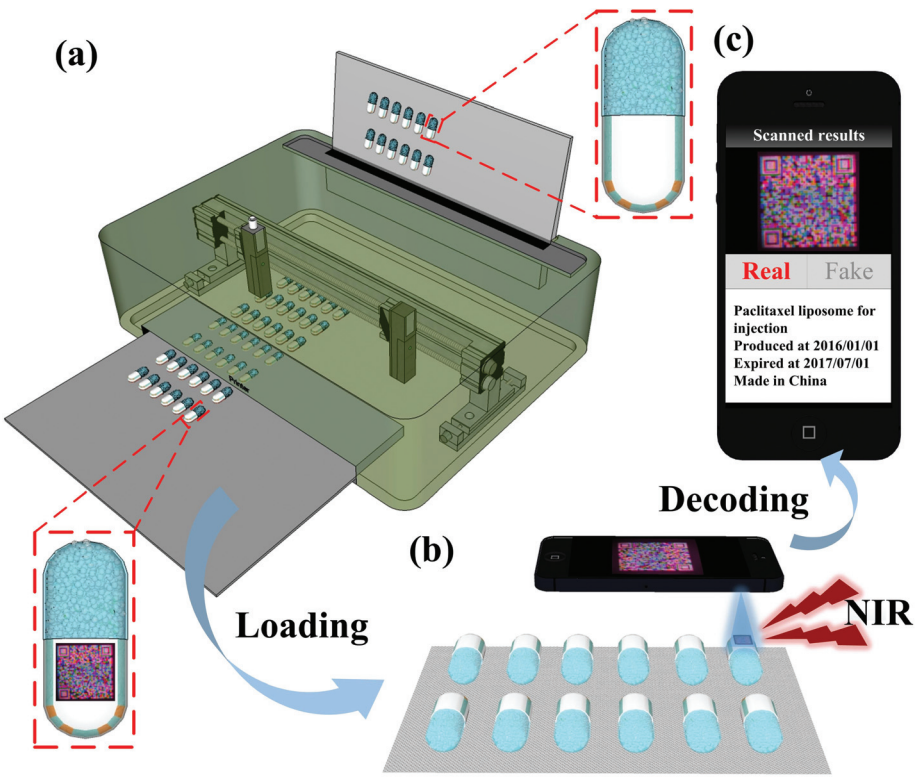

Fig. 1 Schematic image of inkjet printing on capsules and results for identification as well as interpretation using a smart phone. (a) Upconversion fluorescence based 3D QR code printed on capsules using an inkjet printer. (b) Capsule plate loaded drug capsules and upconversion fluorescence based 3D QR code captured by using a smart phone camera upon near infrared light excitation. (c) Decoding of the captured 3D QR code. Real or fake will be suggested based on the decoded information.

Three different colored UCNPs (*i.e.*, RGB) were synthesized for multicolor printing (Fig. 2a–c). To avoid blocking the nozzle of inkjet printer, UCNPs were prepared with a uniform size of 58.5 ± 3.05 nm for red UCNPs ($NaYF_4$:10% Er,2% Tm), 53.7 ± 2.82 nm for green UCNPs ($NaYF_4$:18% Yb,2% Er), and 45.9 ± 2.29 nm for blue UCNPs ($NaYF_4$:25% Yb,0.3% Tm) (Fig. 2d–f), which is smaller than 1/50 of the nozzle diameter (~10 μm) and thus suitable for inkjet printing.[28] Under 980 nm laser excitation, the obtained $NaYF_4$:10% Er,2% Tm, $NaYF_4$:18% Yb,2% Er, and $NaYF_4$:25% Yb,0.3% Tm UCNPs provided red, green, and blue emissions respectively (Fig. 2g–i). To investigate the

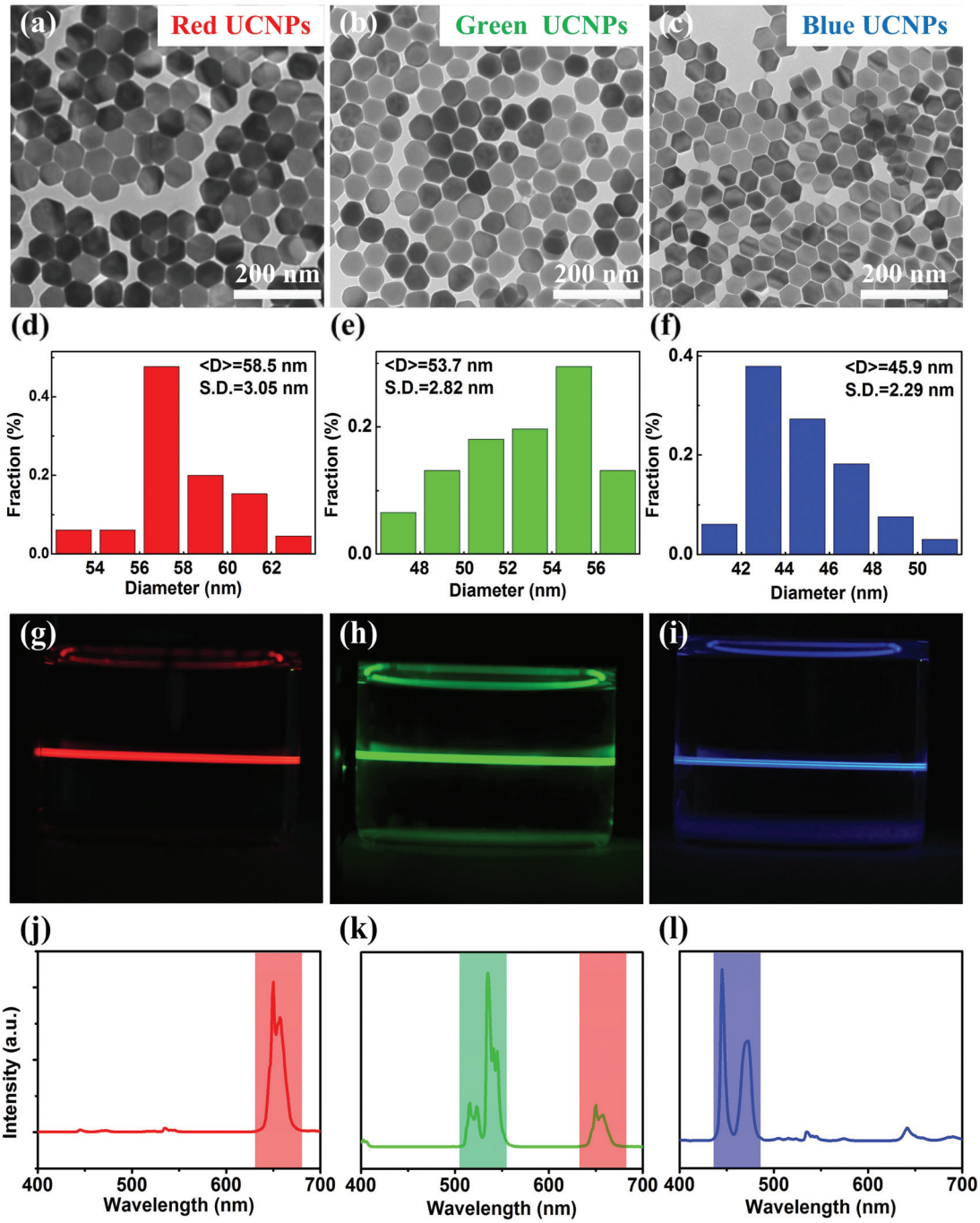

Fig. 2 Characterization of RGB synthesized upconversion nanoparticles. TEM photos of (a) $NaYF_4$:10% Er,2% Tm (red UCNPs), (b) $NaYF_4$:18% Yb,2% Er (green UCNPs), and (c) $NaYF_4$:25% Yb,0.3% Tm (blue UCNPs). Size distribution analysis of (d) red, (e) green, (f) blue UCNPs. Corresponding fluorescence photos of (g) red, (h) green, and (i) blue emissions and fluorescence spectra of (j) red, (k) green, and (l) blue UCNPs under 50 mW mm^{-2} 980 nm laser excitation. The fluorescence photos were taken by dissolving upconversion nanoparticles in cyclohexane solution.

spectral purity, a modified quantification equation is proposed as follows:[29]

$$S_{abc} = \frac{A_a - A_b - A_c}{A_a + A_b + A_c},$$

S_{abc} is used to quantify the spectral purity of emission a, where a could be one of the emission lights of red, green or blue. A_a refers to the emission intensity of a by integrating the corresponding areas in the fluorescence spectrum. Red, green and blue emission areas are suggested from 600 to 700 nm, from 500 to 600 nm, and from 400 to 500 nm, respectively. From the fluorescence spectrum of the three primary color inks (Fig. 2j–l), S_{rgb}, S_{gbr} and S_{brg} were calculated to be 0.90, 0.56 and 0.69, respectively, indicating that all the UCNPs exhibited excellent emission purity, except that green UCNPs also possessed a red emission.

Generally, red, green, and blue are the three primary colors, which can be combined to make full colors. Here, a set of RGB color inks were formulated according to a previous method.[13,30] The RGB additive color model printed on A4 paper was presented under 980 nm laser excitation as designed (Fig. 3a). Secondary colors, yellow, cyan, and magenta are formed by additive overlap of equal perceived intensities of two of the primary colors, whereas white color is formed at the intersection of all three. It is worth noting that the color ink box of the commercial inkjet printer is designed by subtractive three primaries (cyan, magenta, and yellow), which is different in secondary color generation with additive three primaries (red, green, blue). Therefore, we should follow the principle of subtractive three primaries to design the color pattern. To demonstrate that the inkjet printing system is capable of printing multicolored patterns, we printed two color palettes by overlapping blue and red luminescent inks (Fig. 3b), red and green luminescent inks (Fig. 3c) and blue and green luminescent inks (Fig. 3d) at surface coverages of 0%, 25%, 75% and 100% respectively. Utilizing the full color printing technology, various shapes and colorful patterns can be printed, which could be used as anti-counterfeit patterns in the passport or currency. In this study, the major green upconversion emission accompanies slight red emission. To confirm the effect of the red emission on color splitting, we obtained the grayscale image of the red module and green module through the red channel and the mean gray values were measured to be 243 and 8, respectively (Fig. S1†). It should be noted that the mean gray value of the red module is about 30 times higher than that of the green module. This indicates that the accompanying red emission from green UCNPs has no significant effect on color splitting. Noteworthily, the mean gray value of the red module is about 30 times higher than

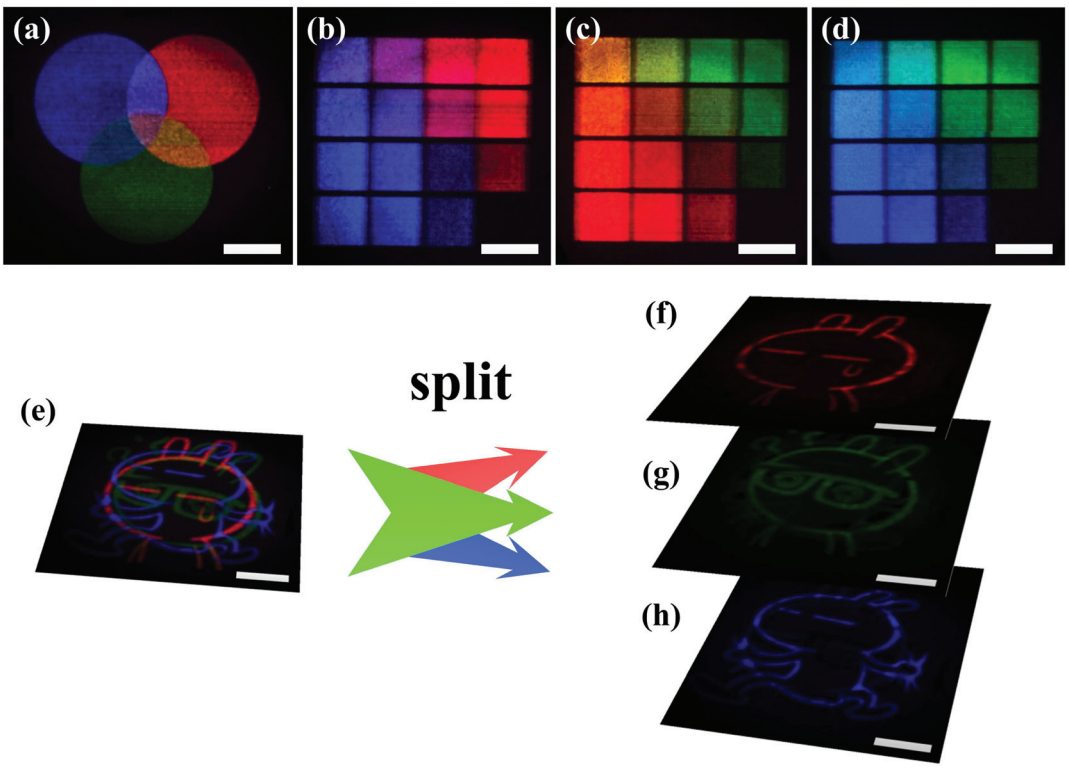

Fig. 3 RGB based multicolor printing. (a) RGB based three primary colors. Color regulation by printing (b) blue and red luminescent inks, (c) red and green luminescent inks and (d) blue and green luminescent inks. Picture under NIR light excitation of the 48 luminescent samples printed on the A4 paper and printed by superposing two luminescent inks at surface coverages of 0%, 25%, 75%, and 100%. (e) Red, green and blue inks printed on the same overlapping surface. The printed pattern could split into three layers according to different color channels, (f) red, (g) green and (h) blue. Scale bar represents 5 mm.

that of the green module. Therefore, we supposed that the accompanying red emission from green UCNPs had very little effect on color splitting. For instance, we printed three different styles of Tuzki using RGB luminescent inks in the same area (Fig. 3h). It is difficult to distinguish these three Tuzki styles when they merged in the same layer. However, the three different styles of the printed multicolor Tuzki pattern can be split using an image software (*e.g.* ImageJ), as shown in Fig. 3e–g, which further proved the feasibility of the 3D QR code.

Nowadays, lots of anti-counterfeit technologies have been devoted to packaging-oriented anti-counterfeiting of drugs. Although they partly protect drugs from forging, they are helpless in preventing the switch of authentic drugs by fake drugs. Such methods are susceptible to fraud by means of imitation and are insufficient for fully authenticating drug ingredients. Here, as a proof of concept for drug tracking anti-counterfeit technology, we developed a upconversion fluorescent based 3D QR code that can be directly printed on the drug surface. To decode the 3D QR code, a specialized smart phone APP was developed. The 3D QR code composed of three primary color QR codes encoded with different information of the drug (Fig. 4a). A programmed process was designed to read the encoded 3D QR code. First, the merged 3D QR code was split into three colored codes through RGB channels (Fig. 4b–d). The obtained QR codes from different RGB channels were of black background and light color modules, which could not be recognized by a common QR code reader. To convert to a commonly readable black/white QR code, the obtained three colored layers were turned to a grayscale image firstly and then to inverted black and white modules by subtracting 255 with a gray value of each pixel before taking the absolute value. Then, the three inverted QR codes were decoded by using common QR code scanners (Fig. 4e–g). Corresponding to the three black/white QR codes, three kinds of information were obtained, including basic drug information, drug photos, and the website of the pharmaceutical company (Fig. 4h–j). Here, we demonstrated the 3D QR code exhibiting a complex code process, strong information capacity and compatibility as a potential anti-counterfeit technology.

To verify the applicability of 3D QR codes for tracking and anti-counterfeiting of drugs, we printed a 3D QR code on the

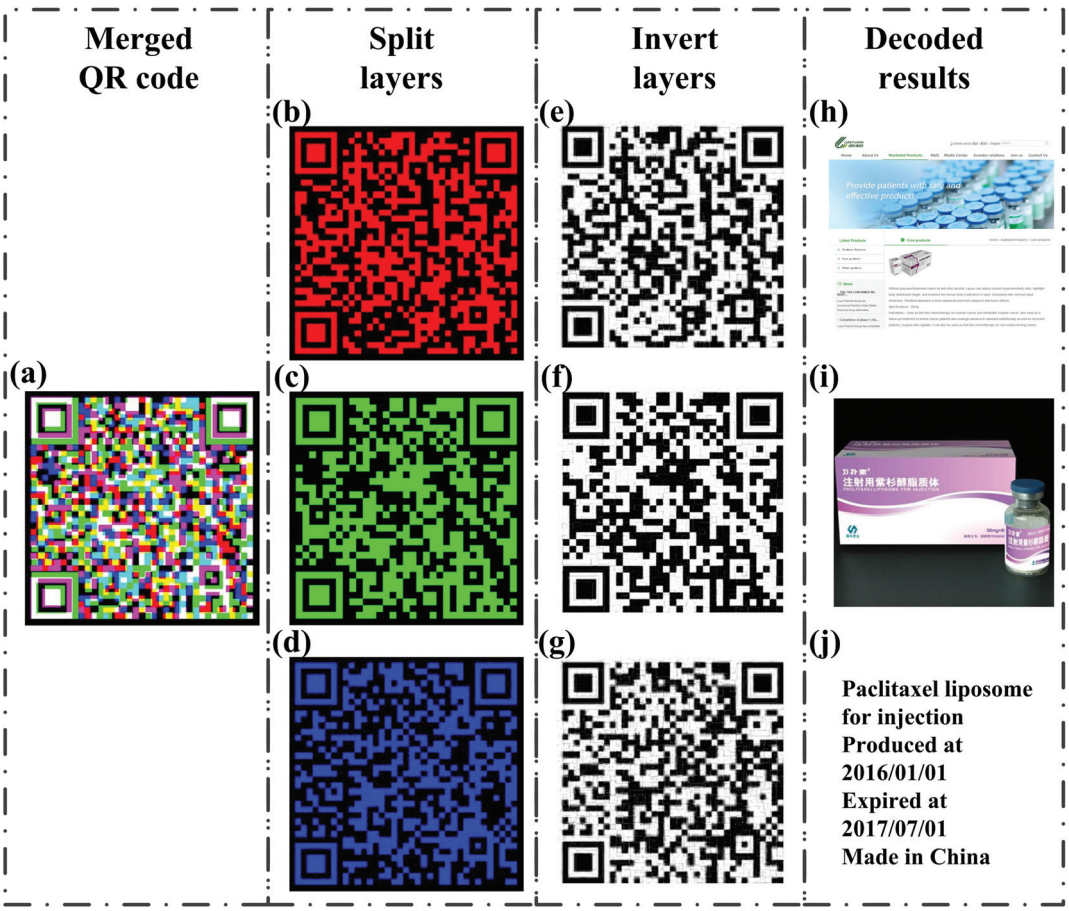

Fig. 4 Principle of the developed smart phone app. (a) 3D QR code merged with three color QR codes. (b) Red layer, (c) green layer and (d) blue layer split from the 3D QR code through RGB color channels. (e–g) Invert layers refer to the corresponding black/white QR codes inverted from mono-color QR codes. The inverted layers are able to directly decode by common QR code apps. The decoded results contain three information types: (h) web link, (i) picture and (j) text.

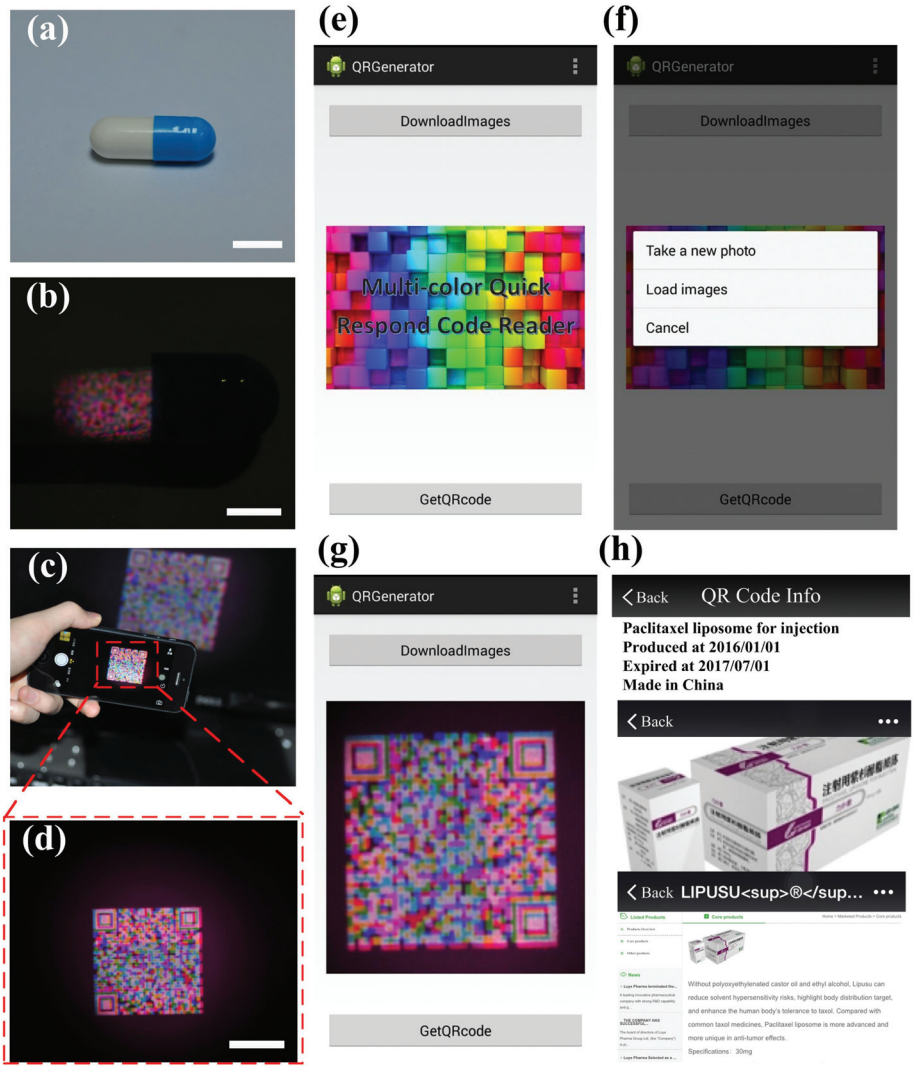

Fig. 5 Decoding process of the 3D QR code printed on the capsule surface using the specialized APP. Photo of a capsule printed with a 3D QR code under (a) room light (scale bar represents 10 mm) and (b) 980 nm laser excitation in a dark room. (c) 3D QR code captured by a smart phone and (d) the enlarged figure. (e) Interface of the specialized smart phone app. (f) Options of 3D QR code input ways under the *Downloadimages* function. (g) 3D QR code loaded into the app. (h) Decoding results of the 3D QR code. Three kinds of results successfully decoded from the 3D QR code are the text of the drug produced date, picture of drug packaging and website of the drug manufacturer. Scale bar represents 5 mm.

surface of a drug capsule (Fig. 5). Due to the printing resolution of the inkjet printer, the size of a QR code should be larger than 1 × 1 cm to obtain a clear pattern required by the subsequent decoding. Therefore, we flattened the capsule to print a 3D QR code and then a drug capsule with the 3D QR code was obtained after recovering its shape using a cotton swab. The obtained drug capsule exhibited no difference with un-printed capsules (Fig. 5a). Under excitation of a 980 nm laser with a power density of 50 mW mm^{-2}, the 3D QR code on the printed drug capsule showed up clearly (Fig. 5b). The printed QR code with 1 × 1 cm size turns out to be a curved surface on the surface of a capsule. Under this condition, the imaging system was unable to capture the whole QR code image. We therefore need to unfold the capsule in order to capture the code. Since the common smart phone camera cannot focus very well in a dark environment for obtaining a high quality 3D QR code, we imaged the 3D QR code using a Nikon D90 camera after unfolding the capsule shell. The image was then transferred to a common smart phone for further decoding (Fig. 5c and d). To obtain a high quality 3D QR code image in a dark environment, a smart phone camera with a laser assisted focus ability can be used or printing the 3D QR code using bright UCNPs. We then used a smart phone to recognize the 3D QR code through a specially developed APP, named a multicolor quick respond code reader (QR generator) (ESI Video 1†). There are two function buttons as *Downloadimage* and *GetQRcode* in the main interface (Fig. 5e). *Downloadimage* is used for loading 3D QR codes, including taking the picture or loading the local image (Fig. 5f). After 3D QR code loading, *GetQRcode* performs its function to decode

the loaded image (Fig. 5g). The encoded information was finally obtained from three black/white QR codes produced by clicking *GetQRcode* (Fig. 5h). The decoding process of the 3D QR code using an Android phone was recorded by a video (ESI Video 1†). The successful decoding of three black/white QR codes from different channels demonstrates that the green upconversion emission that accompanies red emission (Fig. 2k) does not affect the color splitting and subsequent decoding process (Fig. S2†). For expanding its wide applications to other drugs (*e.g.*, tablets, caplets), an eatable thin film could be used as a substrate to print 3D QR codes and then coated onto the surface of drugs. This will be compatible for a variety of drugs while retaining high resolution. Additionally, 3D printing has been used for drug production,[31,32] which provides potential to directly print 3D QR codes at the same time during drug fabrication. However, the usage of an NIR laser as an excitation light source may limit the practical applications of 3D QR codes. A small size, portable and cost-effective NIR LED array as an excitation source to illuminate the anti-counterfeit pattern would be an alternative excitation light source.[33]

As for practical application, the upconversion fluorescent 3D QR code printed capsules should be of no harm and edible. Typically, UCNPs are believed to be safe for biological applications, due to the fact that the chemical elements of the UCNPs may themselves be non-toxic, and secondary toxicity has not yet been observed.[34] However, considering the possible adverse effects caused from the physical and chemical properties of UCNPs as a whole, the toxicity of UCNPs remains to be clarified. Very recently, the toxicity of UCNPs was declared to be concentration dependent.[35] Based on a previous *in vivo* study on PAA coated UCNPs, no apparent adverse effect occurred to the health of mice intravenously injected with a 15–20 mg kg^{-1} dose.[36,37] In our experiment, the 3D QR code on each drug capsule contains approximately 355 ng of UCNPs (calculation details are shown in the ESI†). Assuming that one patient takes three capsules a day, the patient takes approximately 0.39 mg of UCNPs per year and this level is considerably safe based on previous results.

Conclusion

In summary, we reported a high security, high-throughput, user-friendly, designable and low cost inkjet printing-based upconversion fluorescent 3D QR code for drug tracking and anti-counterfeiting. Three colored printing inks of UCNPs with red, green and blue light emissions were separately fabricated. We achieved the precise regulation of printing color and provided a potential full color printing *via* controlling the overlap of the three color inks. Meanwhile, we developed a multilayer printing and splitting technology, which significantly increases the information storage capacity compared with 2D QR codes. As an example of tracking and anti-counterfeiting of drugs, we utilized this technology to print an upconversion fluorescent 3D QR code on drug capsules and followed by decoding with a specialized smart phone APP. The developed anti-counterfeiting technology not only possesses highly advanced anti-counterfeit effect but is also user-friendly and convenient to recognize. Therefore, an upconversion fluorescent based 3D QR code is promising as a powerful tool for drug anti-counterfeiting.

Acknowledgements

This work was financially supported by the National Natural Science Foundation of China (11372243, 11522219, 11402192 and 11532009), the International Science & Technology Cooperation Program of China (2013DFG02930), Fundamental Research Funds for the Central Universities 2016qngz03, National Instrumentation Program (2013YQ190467).

References

1 T. Lancet, Fighting fake drugs: the role of WHO and pharma, *Lancet*, 2011, **377**, 1626.
2 T. Kelesidis and M. E. Falagas, Substandard/Counterfeit Antimicrobial Drugs, *Clin. Microbiol. Rev.*, 2015, **28**, 443–464.
3 R. Cockburn, Death by dilution: when fakes of a GlaxoSmithKline anti-malarial drug turned up in Africa, authorities assumed the drug giant would want to know. Instead, they learned about a huge, evil trade in fake drugs—and about an industry that doesn't want the truth. http://prospect.org/article/death-dilution.
4 C.-W. Yen, H. de Puig, J. O. Tam, J. Gomez-Marquez, I. Bosch, K. Hamad-Schifferli and L. Gehrke, Multicolored silver nanoparticles for multiplexed disease diagnostics: distinguishing dengue, yellow fever, and Ebola viruses, *Lab Chip*, 2015, **15**, 1638–1641.
5 How much does an RFID tag cost today? https://www.rfidjournal.com/faq/show?85.
6 J. Scheuer and Y. Yifat, Holography: Metasurfaces make it practical, *Nat. Nanotechnol.*, 2015, **10**, 296–298.
7 M. M. Jeevan, M. C. William, P. S. May, L. QuocAnh, A. C. Grant and J. K. Jon, Security printing of covert quick response codes using upconverting nanoparticle inks, *Nanotechnology*, 2012, **23**, 395201.
8 O. Graydon, Cryptography: Quick response codes, *Nat. Photonics*, 2013, **7**, 343–343.
9 S. Han, H. J. Bae, J. Kim, S. Shin, S. E. Choi, S. H. Lee, S. Kwon and W. Park, Lithographically Encoded Polymer Microtaggant Using High-Capacity and Error-Correctable QR Code for Anti-Counterfeiting of Drugs, *Adv. Mater.*, 2012, **24**, 5924–5929.
10 M. Ecker and T. Pretsch, Multifunctional poly(ester urethane) laminates with encoded information, *RSC Adv.*, 2014, **4**, 286–292.
11 R. Ameloot, M. B. J. Roeffaers, G. De Cremer, F. Vermoortele, J. Hofkens, B. F. Sels and D. E. De Vos,

Metal–Organic Framework Single Crystals as Photoactive Matrices for the Generation of Metallic Microstructures, *Adv. Mater.*, 2011, **23**, 1788–1791.

12 B. Tyler, M. Jeevan, P. S. May, K. Jon, C. William, A. Krishnamraju, V. Swathi and N. L. QuocAnh, Patterned direct-write and screen-printing of NIR-to-visible upconverting inks for security applications, *Nanotechnology*, 2012, **23**, 185305.

13 M. You, J. Zhong, Y. Hong, Z. Duan, M. Lin and F. Xu, Inkjet printing of upconversion nanoparticles for anti-counterfeit applications, *Nanoscale*, 2015, **7**, 4423–4431.

14 D.-H. Park, W. Jeong, M. Seo, B. J. Park and J.-M. Kim, Inkjet-Printable Amphiphilic Polydiacetylene Precursor for Hydrochromic Imaging on Paper, *Adv. Funct. Mater.*, 2016, **4**, 498–506.

15 M. Singh, H. M. Haverinen, P. Dhagat and G. E. Jabbour, Inkjet printing-process and its applications, *Adv. Mater.*, 2010, **22**, 673–685.

16 Y. Khan, F. J. Pavinatto, M. C. Lin, A. Liao, S. L. Swisher, K. Mann, V. Subramanian, M. M. Maharbiz and A. C. Arias, Inkjet-Printed Flexible Gold Electrode Arrays for Bioelectronic Interfaces, *Adv. Funct. Mater.*, 2016, **7**, 1004–1013.

17 A. V. Yakovlev, V. A. Milichko, V. V. Vinogradov and A. V. Vinogradov, Sol–Gel Assisted Inkjet Hologram Patterning, *Adv. Funct. Mater.*, 2015, **25**, 7375–7380.

18 R. Xie, C. Hong, S. Zhu and D. Tao, Anti-counterfeiting digital watermarking algorithm for printed QR barcode, *Neurocomputing*, 2015, **167**, 625–635.

19 R. Y. Shah, P. N. Prajapati and Y. Agrawal, Anticounterfeit packaging technologies, *J. Adv. Pharm. Technol. Res.*, 2010, **1**, 368–373.

20 G. De Cremer, B. F. Sels, J. I. Hotta, M. B. J. Roeffaers, E. Bartholomeeusen, E. Coutiño-Gonzalez, V. Valtchev, D. E. De Vos, T. Vosch and J. Hofkens, J. Optical Encoding of Silver Zeolite Microcarriers, *Adv. Mater.*, 2010, **22**, 957–960.

21 D.-H. Park, C. J. Han, Y.-G. Shul and J.-H. Choy, Avatar DNA Nanohybrid System in Chip-on-a-Phone, *Sci. Rep.*, 2014, **4**, 4879.

22 M. Lin, Y. Zhao, S. Wang, M. Liu, Z. Duan, Y. Chen, F. Li, F. Xu and T. Lu, Recent advances in synthesis and surface modification of lanthanide-doped upconversion nanoparticles for biomedical applications, *Biotechnol. Adv.*, 2012, **30**, 1551–1561.

23 A. L. Feng, M. L. You, L. Tian, S. Singamaneni, M. Liu, Z. Duan, T. J. Lu, F. Xu and M. Lin, Distance-Dependent Plasmon-Enhanced Fluorescence of Upconversion Nanoparticles using Polyelectrolyte Multilayers as Tunable Spacers, *Sci. Rep.*, 2015, **5**, 7779.

24 Y. Zhang, L. Zhang, R. Deng, J. Tian, Y. Zong, D. Jin and X. Liu, Multicolor Barcoding in a Single Upconversion Crystal, *J. Am. Chem. Soc.*, 2014, **136**, 4893–4896.

25 J. M. Meruga, C. Fountain, J. Kellar, G. Crawford, A. Baride, P. S. May, W. Cross and R. Hoover, Multi-layered covert QR codes for increased capacity and security, *Int. J. Comput. Appl.*, 2015, **37**, 17–27.

26 W. Fan, B. Shen, W. Bu, F. Chen, K. Zhao, S. Zhang, L. Zhou, W. Peng, Q. Xiao, H. Xing, J. Liu, D. Ni, Q. He and J. Shi, Rattle-Structured Multifunctional Nanotheranostics for Synergetic Chemo-/Radiotherapy and Simultaneous Magnetic/Luminescent Dual-Mode Imaging, *J. Am. Chem. Soc.*, 2013, **135**, 6494–6503.

27 J. Birui, L. Min, Y. Minli, Z. Yujin, W. Mingxi, X. Feng, D. Zhenfeng and L. Tianjian, Microbubble embedded with upconversion nanoparticles as a bimodal contrast agent for fluorescence and ultrasound imaging, *Nanotechnology*, 2015, **26**, 345601.

28 F. Torrisi, T. Hasan, W. Wu, Z. Sun, A. Lombardo, T. S. Kulmala, G.-W. Hsieh, S. Jung, F. Bonaccorso, P. J. Paul, D. Chu and A. C. Ferrari, Inkjet-Printed Graphene Electronics, *ACS Nano*, 2012, **6**, 2992–3006.

29 E. M. Chan, G. Han, J. D. Goldberg, D. J. Gargas, A. D. Ostrowski, P. J. Schuck, B. E. Cohen and D. J. Milliron, Combinatorial Discovery of Lanthanide-Doped Nanocrystals with Spectrally Pure Upconverted Emission, *Nano Lett.*, 2012, **12**, 3839–3845.

30 J. M. Meruga, A. Baride, W. Cross, J. J. Kellar and P. S. May, Red-green-blue printing using luminescence-upconversion inks, *J. Mater. Chem. C*, 2014, **2**, 2221–2227.

31 A. Goyanes, A. B. M. Buanz, G. B. Hatton, S. Gaisford and A. W. Basit, 3D printing of modified-release aminosalicylate (4-ASA and 5-ASA) tablets, *Eur. J. Pharm. Biopharm.*, 2015, **89**, 157–162.

32 S. A. Khaled, J. C. Burley, M. R. Alexander and C. J. Roberts, Desktop 3D printing of controlled release pharmaceutical bilayer tablets, *Int. J. Pharm.*, 2014, **461**, 105–111.

33 Y. Zhong, I. Rostami, Z. Wang, H. Dai and Z. Hu, Energy Migration Engineering of Bright Rare-Earth Upconversion Nanoparticles for Excitation by Light-Emitting Diodes, *Adv. Mater.*, 2015, **27**, 6418–6422.

34 A. Gnach, T. Lipinski, A. Bednarkiewicz, J. Rybka and J. A. Capobianco, Upconverting nanoparticles: assessing the toxicity, *Chem. Soc. Rev.*, 2015, **44**, 1561–1584.

35 Y. Sun, W. Feng, P. Yang, C. Huang and F. Li, The biosafety of lanthanide upconversion nanomaterials, *Chem. Soc. Rev.*, 2015, **44**, 1509–1525.

36 L. Xiong, T. Yang, Y. Yang, C. Xu and F. Li, Long-term in vivo biodistribution imaging and toxicity of polyacrylic acid-coated upconversion nanophosphors, *Biomaterials*, 2010, **31**, 7078–7085.

37 L. Cheng, K. Yang, M. Shao, X. Lu and Z. Liu, In vivo pharmacokinetics, long-term biodistribution and toxicology study of functionalized upconversion nanoparticles in mice, *Nanomedicine*, 2011, **6**, 1327–1340.

